Mapping beech (*Fagus sylvatica* L.) forest structure with airborne hyperspectral imagery

Moses Azong Cho[a]*, Andrew, K. Skidmore[b] and Istiak Sobhan[b]

[a]*Council for Scientific and Industrial Research (CSIR), Ecosystem-Earth Observation Unit, P.O. Box 395, Pretoria, South Africa*
[b]*International Institute for Geoinformation Science and Earth Observation. Hengelosestraat 99, P.O. Box 6, 7500 AA Enschede, The Netherlands*

Abstract

The objective of this study was to assess the utility of hyperspectral data in estimating and mapping forest structural parameters including mean diameter-at-breast-height (DBH), mean tree height and tree density of a closed canopy beech forest (*Fagus sylvatica* L). Airborne HyMap images and data on forest structural attributes were collected from the Majella National Park, Italy in July 2004. The predictive performances of normalised difference vegetation indices (NDVI) derived from all possible two-band combinations were evaluated using calibration (n = 33) and test (n = 20) data sets. The potential of partial least squares (PLS) regression was also assessed. New NDVIs based on the contrast between reflectance in the red-edge shoulder (756-820 nm) and the water absorption feature centred at 1200 nm (1172-1320 nm) were found to show higher correlations with the forest structural parameters than standard NDVIs derived from NIR and visible reflectance. PLS regression showed a slight improvement in estimating the beech forest structural attributes compared to NDVI using linear regression models. Mean DBH was the best predicted variable among the stand parameters (calibration R^2 = 0.62 for an exponential model fit and standard error of prediction = 5.12 cm, i.e. 25% of the mean). The predicted map of mean DBH revealed high heterogeneity in the beech forest structure in the study area. The DBH map could be useful to forest management in many ways e.g. thinning of coppice to promote diameter growth, to assess the effects of management on forest structure or to detect changes in the forest structure caused by anthropogenic and natural factors.

Keywords: forest structure; diameter-at-breast height; tree height; tree density, vegetation indices; hyperspectral imagery

1. Introduction

Information about the distribution of forest structural attributes such as tree diameter, basal area, height and density is essential for forest management. For example, thinning of high-density areas could promote diameter growth (Messina, 1992; Baldwin, et al., 2000; Fuhr et al., 2001). Conventional forest inventory data have been collected by means of field surveys. Such surveys are time consuming, labour intensive and expensive when carried out over broad areas (Gower et al., 1999). Remote sensing, using current or anticipated air-spaceborne sensors is widely viewed as a time- and cost-efficient way to proceed with large-scale estimation of forest structural attributes.

A variety of remote sensors have been used in forest inventory studies including passive optical and active (radar and light detection and ranging (LIDAR)) sensors (Nilsson, 1996; Kasischke et al., 1997; Lefsky et al., 1999). The majority of sensors are broadband optical sensors such as Landsat TM/ETM+ and SPOT HVR with three to six broad spectral bands covering the visible, near infrared (NIR) and shortwave infrared (SWIR) regions (Woodcock et al., 1997; Franco-Lopez et al., 2001; Ingram et al., 2005). The most commonly used broadband remote sensing predictors of forest parameters are ratio indices (vegetation indices) computed NIR and visible reflectance. The most known vegetation index is the normalised difference vegetation index (NDVI) developed by Rouse et al. (1974). NDVI is based on the contrast between the maximum absorption in the red due to chlorophyll pigments and the maximum reflectance in the NIR caused by scattering in the leaf mesophyll. For example, with increasing leaf area index (LAI) or canopy thickness, red reflectance decreases as leaf pigments absorb light, while NIR reflectance increases as more leaf layers are present to scatter the radiation (Gates et al., 1965). Thus, passive remote sensing of forest structural attributes such as tree diameter, height, density and biomass indirectly depends on the relationship between these parameters and parameters that have a direct control on the spectral reflectance such as LAI, canopy thickness and canopy biochemistry (Lefsky et al., 1999; Ingram et al., 2005). Broadband NDVI is a poor predictor of tree structural attributes for probably two reasons; firstly, broadband NDVI has been shown to saturate for a certain range of canopy cover or LAI (LAI > 3) (Sellers, 1985; Gao et al., 2000; De Jong et al. 2003) and secondly, broadband indices use average spectral information over broad bandwidths, resulting in loss of critical information, (e.g. for canopy biochemistry) available in specific narrowbands (Gong et al., 2003; Thenkabail et al., 2004).

The advent of narrowband or hyperspectral (imaging spectroscopy) and LIDAR sensors has raised new expectations about the possibilities of improving the estimation of forest structural parameters. One hand, imaging spectroscopy can provide information on the cover, abundance and concentration of biochemicals and on the other hand, LIDAR can provide information on the cover, height, shape and architecture of vegetation (Asner et al. 2007). The use of imaging spectroscopy for forest stand structural estimation is based on the assumption that increased identification of particular spectral features associated with narrowbands could improve estimation of forest attributes compared to broadband sensors (Lefsky et al., 2001; Lee et al., 2004). However, it is difficult to infer from existing literature whether hyperspectral sensors provide an improvement over multispectral sensors for remote sensing of forest structural attributes. For example, Lefsky et al. (2001) observed a slight increase in the ability of Airborne Visible-Infrared Imaging Spectrometer (AVIRIS) to predict forest stand attributes relative to single date

Landsat TM data, but a better performance of multitemporal Landsat TM data. Gong et al (2003) showed that indices involving NIR and SWIR Hyperion bands were better than NIR-red indices for LAI estimation. Lee et al. (2004) found no improvement of AVIRIS NDVI over ETM+ NDVI for LAI estimation. The potential of hyperspectral data for estimating forest stand attributes for different ecosystems and seasons is not fully understood.

The objective of this study was therefore, to assess the utility of hyperspectral data in estimating and mapping forest structural parameters including mean diameter-at-breast-height (DBH), mean tree height and tree density of a closed canopy beech forest (*Fagus sylvatica* L).

Insert Fig. 1

2. Material and methods

2.1. Study site

The study site was located in Majella National Park, Italy (latitude 41°52' to 42°14'N, longitude 13°50' to 13°14'E) covering an area of 74095 ha (Fig. 1). The Park extends into the southern part of Abruzzo, at a distance of 40 km from the Adriatic Sea. This region is situated in the massifs of the Apennines. The park is characterised by several mountain peaks, the highest being mount Amaro (2794 m). The region is characterised by Mediterranean climate: hot and dry summers and cool and wet winters. The specific study site (latitude 41°49' to 42°14'N, longitude 13°57' to 14°3'E) is situated between mounts Majella and Morrone to the east and west, respectively. It covers an area of 40 by 5.5 km.

The Majella beech forest is located at an altitude range of about 1200-1800 m. Over the last 60 years, depopulation, changes in the socio-economic conditions and the creation of the National Park in 1995 have led to a pronounced drop in the local demand for small size timber, firewood and charcoal (Ciancio et al., 2006). As a consequence, many coppices are returning to high forest. However, a combination of thinning and the occurrence of avalanches in Majella have given rise to a compound coppice, which is a mixture of coppice and high forest.

2. 2. Image acquisition and processing

Airborne HyMap data of the study site were obtained on 15 July 2004. The flight was carried out by DLR, Germany's Aerospace Research Centre and Space Agency. The HyMap sensor comprised 126 wavebands, operating over the wavelength range 442 nm to 2485 nm, with average spectral resolutions of 15 nm (442 nm to 1313 nm), 13 nm (1409 nm to 1800 nm) and 17 nm (1953 nm to 2485 nm). The spatial resolution of the data was 4 m. The data were collected at solar noon. The specific study site was covered by four image strips, each covering an area of about 40 km by 2.3 km. The solar zenith and azimuth angles for the image strips range between 30-33.7° and 111.5-121°, respectively. The image strips were atmospherically and geometrically corrected by DLR. The on-board navigation system used for geometric correction was a C-MIGITS II (Miniature Integrated GPS/INS Tactical System) which has a 2.5 m accuracy in the x-y plane and an accuracy of 3m in the z-plane. The atmospheric correction was carried out using ATCOR4-r (Atmospheric/Topographic Correctionrugged terrain). ATCOR4 is based on MODTRAN-4 radiative transfer code (Richter and Schlapfer, 2002).

2.3. Field measurements of forest stand attributes (mean DBH, mean tree height and tree density)

Field data for DBH, height and number of trees were collected from 56 plots within the flight strips between 28 June and 16 July 2004. Random sampling with clustering was adopted in the study because of the difficult nature of the terrain. That is, 20 coordinate points were randomly generated using ArcGIS software. Measurements were made from each randomly selected plot (30 m by 30 m) and from two to three other plots at about 150 and 300 m away in a randomly chosen direction. Plots were located in the field using a Garmin (etrex vista Cx) GPS (5 to 8 m accuracy in the forest). Data was only collected from closed canopy forest in homogeneous areas (i.e. homogeneous in DBH and tree density). This ensured that inconsistencies in the spectral data potentially caused by differences between the field GPS accuracy and in-flight GPS reading could be minimised. The DBH of all trees above 7 cm was measured while the tree heights of five to ten trees were measured using a Haga meter. The mean DBH and height were subsequently calculated per plot. Tree density was calculated as the number of trees per hectare.

2.4. Data analysis

The forest parameters were predicted as continuous variables rather than as a set of discrete classes. Lefsky (2001) argues that the continuous variable approach offers flexibility because the predictions can be used directly or arranged into multiple sets of classes that match varying purposes.

A 7-by-7 pixels window (28 m-by-28 m) was used to collect image spectra from each sample plot in order to avoid including pixels located outside the plot (30 m by 30 m). An average spectrum was subsequently calculated for each plot. Three plots out of the 56 sampled plots were present in areas of shadow and were therefore not considered in the analysis. The data were randomly split into the training or calibration (n = 33) and test (n = 20) sets. The predictive capabilities of linear regression models based on spectral indices and partial least squares (PLS) regression were investigated. Regression analyses were performed on the calibration set. Empirical validations of the calibration models were carried out using the test set. The predictive performances of the various models were estimated and compared using the coefficient of determination (R^2) for calibration and validation, the standard error of calibration (SEC, Eq. 1) and standard error of prediction (SEP) based on the independent test data.

$$SEC = \sqrt{\frac{\sum_{i=1}^{n}(y - y')^2}{n}} \tag{1}$$

where y = measured DBH or height or density, y' = predicted DBH or height or density and n = number of observations.

(i) Vegetation indices

Narrowband NDVIs (Eq. 2) were derived from all possible two-band combinations involving 126 bands of HyMap spectrum using the calibration data. This resulted into 15876 (i.e. 126*126) NDVIs for each spectrum.

$$\text{NDVI}_{(i,j,n)} = (\text{R}_{(i,n)}\text{-R}_{(j,n)})/(\text{R}_{(i,n)}\text{+R}_{(j,n)}) \tag{2}$$

where $R_{(i,n)}$ and $R_{(j,n)}$ are the reflectance of any two band, and n = number of samples.

Linear regression analyses were performed between each NDVI with each tree structural parameter (mean DBH, mean height and tree density). The NDVIs that yielded the highest calibration coefficient of determination (R^2) were subsequently selected for assessing their predictive capability on the independent data set. Although the data for mean DBH, mean height and density were not normally distributed as will be demonstrated later in this paper; the use of parametric regression techniques was justified assuming normality under the central limit theorem ($n \geq 30$). Furthermore, as a means of dealing with the problem of non-normal distribution of the data, a bootstrap procedure was adopted in computing the correlation coefficients for the linear regression analysis. That is, the intercept and slope for each regression equation consisted of mean values derived from using 1000 resamples (replicates) created by repeated sampling with replacement from the calibration data sets. Each resample was of the same size as the original calibration data.

To compare the prediction accuracies for a broadband sensor like Landsat TM, the HyMap data was resampled to the spectral coverage of Landsat TM, with band centres at 481 nm, 568 nm, 665 nm, 831 nm, 1653 nm and 2220 nm. The resampling was conducted using a Gaussian built-in function in ENVI (Environment for Visualising Images, Research System, Inc.) software. All possible Landsat TM two-band NDVIs were subsequently assess for predicting mean DBH, mean height and tree density.

(ii) Partial least squares regression (PLS)

PLS regression was applied in this study to test whether the use of several hyperspectral bands improves the prediction of stand attributes when compared to two-band vegetation indices. PLS regression is a multivariate statistical technique that is widely used in chemometrics to deal with the problem of collinearity among several spectral bands. PLS regression reduces the large number of measured collinear spectral variables to a few non-correlated latent variables (Geladi et al., 1999; Geladi and Kowalski, 1986; Hansen and Schjoerring, 2003). In this sense, PLS regression is closely related to principal component regression (Geladi and Kowalski, 1986; Geladi et al., 1999). But instead of first decomposing the spectra into a set of eigenvectors and scores and regressing them against the response variables as a separate step, PLS regression actually uses the response variable information during the decomposition process. Further information on the PLS regression can be obtained in Geladi and Kowalski (1986).

It has been shown that variable selection enhances the predictive performance of PLS regression (Kubinyi, 1996; Cho et al. 2007, Darvishzadeh et al. 2008). A sub-objective therefore, was to test PLS models based on all the HyMap bands and on a small number of selected bands. The selection was based on bands related to leaf chlorophyll, LAI and leaf mass (Table 1). The utility of the bands represented in Table 1 has been demonstrated in two other studies, i.e. Cho (2007) and Darvishzadeh et al. (2008) for estimating grass biomass and LAI, respectively.

Insert Table 1

Before the PLS regression models were developed, the spectra and forest parameters were mean-centred, i.e. the average value for each variable was calculated from the calibration set and then subtracted from each corresponding variable. The root mean square error of leave-one-out cross validation (RMSECV) was used as a selection criterion to choose the optimum number of latent variables (PLS factors) for predicting the forest structural parameters (Geladi and Kowalski, 1986; Viscarra Rossel, 2005). The RMSECV was determined for each cross-validation phase. The number of factors which yielded the lowest RMSECV was used to develop the calibration equations. The analyses were carried out using STATISTICA software (StatSoft, Inc.) and ParLes software developed by Viscarra Rossel (2008).

Insert table 2

3. Results

3.1. Descriptive statistics of the beech forest structural parameters

The descriptive statistics of the forest structural parameters are presented in Table 2. Each parameter showed a positive skewness indicating a bias of the distribution towards higher values. The Shapiro-Wilk test was used to test the data for normality, the hypotheses were, the null hypothesis (H_0): data follow a normal distribution versus the alternate hypothesis (H_1): the data do not follow a normal distribution. The null hypothesis was rejected in all cases ($p<0.05$). Consequently, the intercorrelations between parameters were analysed using a non-parametric test (Spearman's rank correlation test). Mean DBH was positively related to height ($r = 0.70$, $p<0.05$) but negatively related to tree density ($r = -0.91$, $p<0.05$). Mean height was less highly related to density ($r = -0.60$) than the mean DBH.

Insert Fig. 2

3.2. Relationships between the beech forest structural parameters and individual band reflectance

The relationships between forest parameters and individual band reflectance were analysed using Spearman's rank correlation test. Statistically significant ($p<0.05$) correlations were predominantly observed in the NIR (Fig. 2). The relationships were significant in the following regions:

- Mean DBH and tree density: 711-1342 nm
- Mean height: 528-589 nm, 725-1405 nm, 1530-1806 nm and 2257 nm.

Mean DBH and mean height were negatively correlated with the NIR bands, while density was positively correlated with the NIR bands. This means that higher tree density results in higher NIR reflectance.

Insert Fig. 3.

3.3. Predicting beech forest structural parameters

3.3.1. Using vegetation indices

The contour plots in Fig. 3 show the correlation (R^2) patterns between NDVIs computed from all possible two-band combinations and the three tree structural parameters under study. The contour plots allowed for the identification of the most sensitive NDVIs to mean DBH, mean height and tree density. Similar correlation patterns were observed for mean DBH and tree density. The highest correlations (R^2>0.4) for mean DBH and tree density were observed when these parameters were correlated with NDVIs computed from bands in the red-edge shoulder (756-820 nm) in combination with bands in the water absorption feature centred at 1200 nm (1172-1320 nm). Mean tree height showed the lowest correlations (R^2<0.35) with the various NDVIs among the three structural parameters. The highest correlations for tree height were observed for NDVIs involving bands located in 1172-1301 nm range.

Insert Table 3.
Insert Table 4

The predictive capabilities of the best NDVI combinations for each tree parameter are shown in Table 3. Among all three stand attributes studied, mean DBH was the best predicted parameter using linear regression analysis. Average prediction errors of 27.7%, 35.5% and 48.2% were, respectively obtained for mean DBH, mean height and tree density when the best NDVIs were considered. The standard NDVI involving NIR (831 nm) and red (665 nm) bands showed higher prediction errors when compared to the best NDVIs for all tree structural attribute; 33%, 36% and 54% for mean DBH, mean tree height and tree density, respectively (Table 3). Similar prediction accuracies were observed for the standard NDVI computed from the spectrally resampled (simulated Landsat TM) data (see Table 4).

The scatter plots in Fig.4 illustrate the nature of the relationship between mean DBH and the best NDVI involving bands at 771 nm and 1287 nm and the standard NDVI computed from the simulated Landsat TM data. The graphs showed a 'local bias' along the 1:1 line between the predicted versus the actual DBH values. The low values are predicted high and high values are predicted low, indicating non-linearity in the relationship between DBH and NDVI. NDVI appeared to saturate for mean DBH above 30 cm. For example, when an exponential model fit was used in the regression analysis (Fig.5), the calibration R^2 for the best NDVI increased from 0.51 to 0.62 (22% increase), while the SEP decreased from 5.50 cm to 5.12 cm (7% decrease).

Insert Fig. 5
Insert Table 5

3.3.2. Using partial least squares regression

The predictive performances of PLS regression based on all the HyMap bands and selected bands were basically similar (Table 5). Like in the case of spectral indices, mean DBH was the best-predicted parameter, followed by mean height and lastly density. However, there was a slight improvement in the prediction accuracy of the various parameters when compared with results for the best NDVIs. Percentage prediction errors of 26.8%, 33.2% and 46.4% were observed for mean DBH, mean height and tree density, respectively. As was the case with the regression model involving NDVIs, the results of the PLS modelling showed a strong 'local bias' in the calibration and test data (Fig. 6). The higher values were predicted low and the low values were predicted high.

Insert Fig. 6

3.4. Mapping forest structure

The Majella beech forest structure was mapped using the best-predicted parameter, i.e., mean DBH. Mean DBH map was produced using the exponential model (see Fig.5) derived from the calibration between mean DBH and the best NDVI combinations i.e. 771 and 1287 nm. Prior to the mapping of mean DBH, a mask of beech forest areas was created from the HyMap image strips using NDVI threshold values, thus eliminating areas occupied by other land-cover types (mainly grasslands and housing areas). The predicted map of mean DBH is presented in Fig. 7. The map of DBH shows high heterogeneity of DBH within the various forest patches. There is no clear effect of altitude on the forest structure.

Insert Fig. 7.

4. Discussion and conclusions

4.1. Predicting beech forest structural parameters

New NDVIs based on the contrast between reflectance in the red-edge shoulder (756-820 nm) and the water absorption feature centred at 1200 nm (1172-1320 nm) were found to show higher correlations with forest structural parameters than standard NDVIs derived from NIR and visible reflectance. Leaf water content thus, appears to be the limiting factor determining differences between forest stands of varying DBH or density rather than leaf chlorophyll content. We hypothesize that the nature of the relationship between the various NDVIs and forest structural attributes could depend on the beech forest phenology. Based on the results of this study, remote sensing of beech forest structure is recommended during periods of the year when water availability is a limiting factor. A drawback of models that are seasonal dependent is that they are not transferable between sites or season (Foody et al. 2003).

Related studies on estimating grass biophysical properties (LAI, biomass) generally show that NDVIs computed from red-edge reflectance (700-800 nm) provide higher accuracies of estimation compared to the standard NDVIs (Mutanga and Skidmore, 2004, Cho et al. 2007, Cho and Skidmore, in press). The red-edge indices have shown high sensitivity sensitive to leaf chlorophyll, nitrogen and grass biomass (Vogelmann et al., 1993; Carter, 1994; Cho et al., 2006, Cho et al. 2008). In this study however, the red-edge indices, showed poor predictive capabilities for forest structural parameters. Their predictive capability for the tree structural parameters could have been hampered by the fact that the beech forest structural attributes were weakly correlated with the chlorophyll (visible) spectrum (see Fig. 1).

PLS regression, the multivariate statistical method adopted in this study, showed a slight improvement in estimating the beech forest structural attributes compared with univariate regression models based on vegetation indices. PLS regression has rarely been applied for estimating forest attributes from remotely sensed data. However, several other studies have shown that PLS regression improves grass biomass or LAI estimation (Hansen and Schjoerring, 2003; Cho et al. 2007; Darvishzadeh et al. 2008) compared to univariate techniques involving vegetation indices. PLS regression models based on a few selected bands and on all HyMap bands produced similar calibration and validation accuracies. The spectral information content required for estimating forest structural parameters might be contained in a few narrowbands. An optimum band selection procedure could therefore, enhance model parsimony.

The prediction of the forest structural attributes in this study reveals the phenomenon of 'local bias'. Local bias occurs when high values of the response variable are predicted low and the low values predicted high (Geladi et al, 1999). Geladi et al. (1999) argue that some of the deviations from the diagonal representing the 1:1 relationship between the predicted and actual values may be attributed to random noise. However, when the bias becomes systematic, as was the case in our study, it may be attributed to non-linearity in the true physical relationship (Geladi et al. 1998). The saturation of the spectral signal in dense and multi-layered canopy cover is a well-known phenomenon (Sellers, 1985; Gao et al., 2000).

Overall, mean DBH was the best predicted using the various statistical methods compared to mean height and tree density. It should be stated again that imaging spectroscopy of forest structural attributes such as tree diameter, height, density and biomass indirectly depends on the relationship between these parameters and parameters that have a direct control on the spectral reflectance such as LAI, canopy thickness and canopy biochemistry (Lefsky et al., 1999; Ingram et al., 2005). Multispectral (broadband) features are poor predictor of canopy biochemistry. This probably explains why spectral degradation from HyMap to Landsat band setting lowered the ability to accurately predict the forest stand attributes. Finally, LIDAR remote sensing has proven useful in providing accurate information on tree height than imaging spectroscopy (Asner et al. 2007). Thus, the combination of LIDAR and imaging spectroscopy could provide more accurate information on beech DBH and height, two parameters important for estimating forest biomass (De Jong et al. 2003).

4.2. Predictive maps of mean DBH and implications for beech forest management in the Majella National Park

The predicted map of mean DBH revealed high heterogeneity in the beech forest structure in the study area. This pattern could be attributed to the forest management practice in the park. A combination of thinning and the occurrence of avalanches in the Majella National Park, have given rise to a compound coppice, which is a mixture of coppice and high beech forest. The DBH map could be useful to forest management in many ways e.g. thinning of coppice to promote diameter growth (tree density was negatively related to DBH), to assess the effects of management on forest structure or to detect changes in the forest structure caused by anthropogenic and natural factors.

Acknowledgments

The International Institute for Geo-Information Science and Earth Observation (ITC) provided financial support for this study. We extend our gratitude to Fabio Corsi, Roshanak Darvishzadeh and Jane Bemigisha all colleagues of the Natural Resources Department of ITC for their assistance during the field campaign. We also appreciate the generous help provided by many people at the Majella National Park, Italy and particularly by Dr Theodoro Andrisano.

References

Asner, G.P., Knapp, D.E., Kennedy-Bowdoin, T., Jones, M.O., Martin, R.E., Boardman, J. and Field, C.B., 2007. Carnegie Airborne Observatory: in-flight fusion of hyperspectral imaging and waveform light detection and ranging (wLiDAR) for three-dimensional studies of ecosystems. Journal of Applied Remote Sensing, 1:1:21.

Baldwin Jr, V.C., Peterson, K.D., ClarkIII, A, Ferguson, R.B., Strub, M.R., Bower. D.R., 2000. The effects of spacing and thinning on stand and tree characteristics of 38-year-old Loblolly Pine. Forest Ecology and Management, 137(1-3): 91-102.

Carter, G.A., 1994. Ratios of leaf reflectance in narrow wavebands as indicator of plant stress. International Journal of remote sensing, 15: 697-704.

Cho, M.A. and Skidmore, A.K. (in press). Hyperspectral predictors for monitoring biomass production in Mediterranean mountain grasslands:Majella National Park, Italy. International Journal of Remote Sensing.

Cho, M.A. and Skidmore, A.K., 2006. A new technique for extracting the red edge position from hyperspectral data: The linear extrapolation method. Remote Sensing of Environment, 101(2): 181-193.

Cho, M.A., Skidmore, A.K. and Atzberger, C., 2008. Towards red edge positions less sensitive to canopy biophysical parameters using properties optique spectrales des feuiles (PROSPECT) and scattering by arbitrarily inclined leaves (SAILH) simulated data. International Journal of Remote Sensing, 29 (8), 2241-2255.

Cho, M.A., Skidmore, A.K., Corsi, F., van Wieren, S.E. and Sobhan, I., 2007. Estimation of green grass/herb biomass from airborne hyperspectral imagery using spectral indices and partial least squares regression. International Journal of Applied Earth Observation and Geoinformation, 9:414-424.

Ciancio O., Corona, P., Lamonaca, A., Portoghesi, L. and Travaglini, D., 2006. Conversion of clearcut beech coppices into high forests with continuous cover: A case study in central Italy. Forest Ecology and Management, 224: 235-240.

Curran, P.J., 1989. Remote sensing of foliar chemistry. Remote Sensing of Environment, 30(3): 271-278.

Darvishzadeh, R., Skidmore, A., Scherf, M., Atzberger, C., Corsi, F. and Cho, M., 2008. LAI and chlorophyll estimation for a heterogeneous grassland using hyperspectral measurements. ISPRS Journal of Photogrammetry & Remote Sensing, 63, 409-426.

De Jong, S.M., Pebesma, E.J. and Lacaze, B., 2003. Above-ground biomass assessment of Mediterranean forests using airborne imaging spectrometry: the DAIS Peyne experiment. International Journal of Remote Sensing, 24(7): 1505-1520.

Foody, G.M., Boyd, D.S. and Cutler, M.E.J., 2003. Predictive relations of tropical forest biomass from Landsat TM data and their transferability between regions. Remote Sensing of Environment, 85(4): 463-474.

Franco-Lopez, H., Ek, A.R. and Bauer, M.E., 2001. Estimation and mapping of forest stand density, volume, and cover type using the k-nearest neighbors method. Remote Sensing of Environment, 77(3): 251-274.

Fuhr, M., Nasi, R. and Delegue, M.-A., 2001. Vegetation structure, floristic composition and growth characteristics of Aucoumea klaineana Pierre stands as influenced by stand age and thinning. Forest Ecology and Management, 140(2-3): 117-132.

Gao, X., Huete, A.R., Ni, W. and Miura, T., 2000. Optical-biophysical relationships of vegetation spectra without background contamination. Remote Sensing of Environment, 74: 609-620.

Gates, D.M., Keegan, H.J., Schleter, J.C. and Weidner, V.R., 1965. Spectral properties of plants. Applied Optics, 4(1): 11-20.

Geladi, P., Hadjiiski, L. and Hopke, P., 1999. Multiple regression for environmental data: nonlinearities and prediction bias. Chemometrics and Intelligent Laboratory Systems, 47(2): 165-173.

Geladi, P. and Kowalski, B.R., 1986. Partial least-squares regression: a tutorial. Analytica Chimica Acta, 185: 1-17.

Gitelson, A.A. and Merzlyak, M.N., 1997, Remote estimation of chlorophyll content in higher plant leaves. International Journal of Remote Sensing, 18(12): 2691-2697.

Gong, P., Pu, R., Biging, G.S. and Larrieu, M.R., 2003. Estimation of forest leaf area index using vegetation indices derived from hyperion hyperspectral Data. IEEE Transactions on Geoscience and Remote Sensing, 41: 1355–1362.

Gower, S.T., Kucharik, C.J. and Norman, J.M., 1999. Direct and Indirect Estimation of Leaf Area Index, fAPAR, and Net Primary Production of Terrestrial Ecosystems. Remote Sensing of Environment, 70(1): 29-51.

Guyot, G. and Baret, F., 1988. Utilisation de la haute résolution spectrale pour suivre l'état des couverts végétaux, Proceedings of the 4th International colloquium on spectral signatures of objects in remote sensing. ESA SP-287, Aussois, France, pp. 279-286.

Hansen, P.M. and Schjoerring, J.K., 2003. Reflectance measurement of canopy biomass and nitrogen status in wheat crops using normalized difference vegetation indices and partial least squares regression. Remote Sensing of Environment, 86: 542-553.

Horler, D.N.H., Dockray, M. and Barber, J., 1983. The red edge of plant leaf reflectance. International Journal of Remote Sensing, 4(2): 273-288.

Ingram, J.C., Dawson, T.P. and Whittaker, R.J., 2005. Mapping tropical forest structure in southeastern Madagascar using remote sensing and artificial neural networks. Remote Sensing of Environment, 94(4): 491-507.

Kasischke, E.S., Melack, J.M., and Dobson, M.C., 1997. The use of imaging radar for ecological applications – a review. Remote Sensing of Environment, 59:141-156.

Kubinyi, H., 1996. Evolutionary variable selection in regression and PLS analyses. Journal of Chemometrics, 10: 119– 133.

Lee, K.-S., Cohen, W.B., Kennedy, R.E., Maiersperger, T.K. and Gower, S.T., 2004. Hyperspectral versus multispectral data for estimating leaf area index in four different biomes. Remote Sensing of Environment, 91(3-4): 508-520.

Lefsky, M.A., Cohen, W.B., Ackerm S.A., Spies, T.A, Parker, G.G. and Harding, D., 1999. Lidar Remote Sensing of the Canopy Structure and Biophysical Properties of Douglas-Fir Western Hemlock Forests. Remote Sensing of Environment, 70(3): 339-361.

Lefsky, M.A. Cohen, W.B. and Spies, T.A. 2001. An evaluation of alternative remote sensing products for forest inventory, monitoring and mapping of Douglas-fir forests in Western Oregon. Canadian Journal of Forest Research, 31(2): 78-87.

Messina, M.G., 1992. Response of Eucalyptus regnans F. Muell to thinning and urea fertilization in New Zealand. Forest Ecology and Management, 51(4): 269-283.

Mutanga, O. and Skidmore, A.K., 2004. Narrow band vegetation indices overcome the saturation problem in biomass estimation. International Journal of Remote Sensing, 25: 1-16.
Nilsson, M., 1996. Estimation of tree height and stand volume using an airborne lidar system. Remote Sensing of Environment, 56:1-7.
Richter, R. and Schlapfer, D., 2002. Geo-atmospheric processing of airborne imaging spectrometry data. Part 2: atmospheric/topographic correction. International Journal of Remote Sensing, 23: 2631-2649.
Rouse, J.W., Haas, R.H., Schell, J.A., Deering, D.W. and Harlan, J.C., 1974. Monitoring the vernal advancement and retrogradation of natural vegetation, NASA/GSFC, Type III Final Report, M.D. Greenbelt, pp. 371.
Sellers, P.J., 1985. Canopy reflectance, photosynthesis and transpiration. International Journal of Remote Sensing, 6(8): 1335-1372.
Thenkabail, P.S., Enclona, E.A., Ashton, M.S. and Van Der Meer, B., 2004. Accuracy assessments of hyperspectral waveband performance for vegetation analysis applications. Remote Sensing of Environment, 91(3-4): 354-376.
Viscarra Rossel, R.A., 2008. ParLeS: Software for chemometric analysis of spectroscopic data. Chemometrics and Intelligent Laboratory Systems, 90: 72-83.
Vogelmann, J.E., Rock, B.N. and Moss, D.M., 1993. Red-edge spectral measurements from sugar maple leaves. International Journal of Remote Sensing, 14: 1563-1575.
Woodcock, C.E. Collins, J., Jakabhazy, V.D., Li, X., Macomber, S.A. and Wu, Y., 1997. Inversion of the Li-Strahler canopy reflectance model for mapping forest structure. IEEE Transactions on Geoscience and Remote Sensing, 35(2): 405-414.

List of figures

Fig.1. Location of the Majella National Park, Italy and HyMap flight lines.

Fig.2. Correlograms of mean diameter-at-breast-height (DBH), mean height and tree density.

Fig.3. Contour plots showing the correlation (R^2) between normalised difference vegetation index (NDVI) values calculated from all possible band combinations (442-2482 nm) and (A) mean diameter-at-breast height (DBH), (B) mean height and (C) tree density of beech forest (*Fagus sylvatica*).

Fig.4. (i) Calibration (n =33) and (ii) independent validation (n = 20) results for predicting beech forest mean diameter-at-breast height using (DBH) (A) best HyMap NDVI computed from 771 and 1287 nm and (B) standard NDVI computed from 831 and 665 nm. SEC = standard error of calibration and SEP = standard error of prediction.

Fig.5. (i) Predicting beech forest mean diameter-at-breast height (DBH) using an exponential model fit between DBH and NDVI computed from 771 and 1287 nm. SEC = standard error of calibration and SEP = standard error of prediction.

Fig.6. Relationship between predicted and actual mean tree diameter-at-breast-height (DBH) for (A) calibration and (B) validation analyses using partial least squares regression. SEC = standard error of calibration, SEP = standard error of prediction. I, II and III indicate low medium and high DBH classes.

Fig.7. Predicted maps of beech forest mean tree diameter-at-breast-height in the Majella National Park, Italy using NDVI computed from 771 and 1287 nm

Figure
Click here to download high resolution image

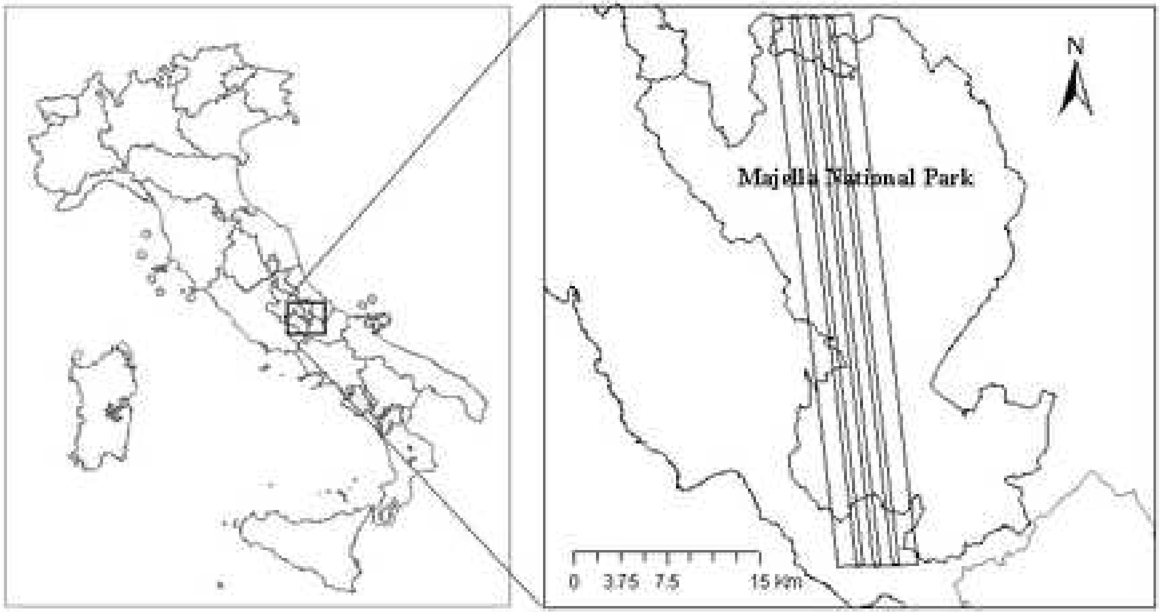

Figure

Click here to download high resolution image

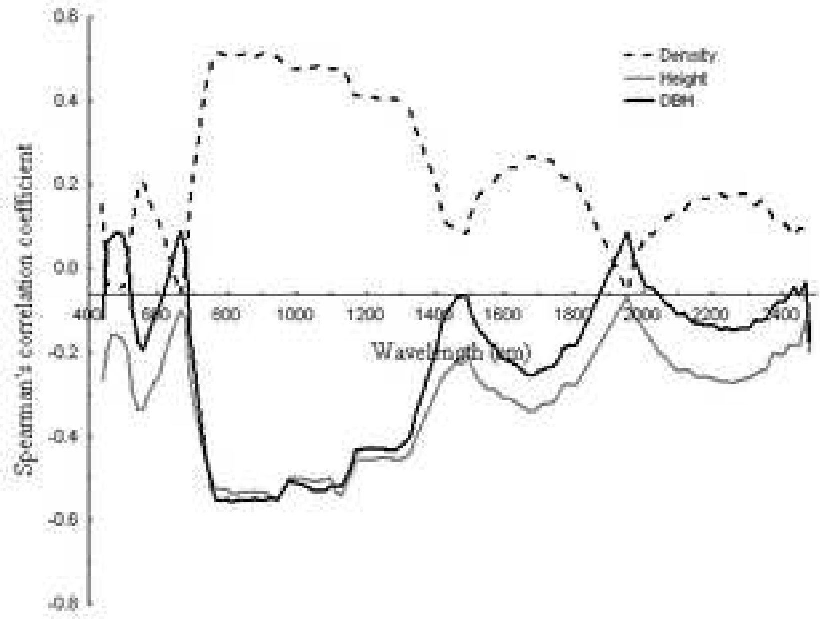

Figure
[Click here to download high resolution image]

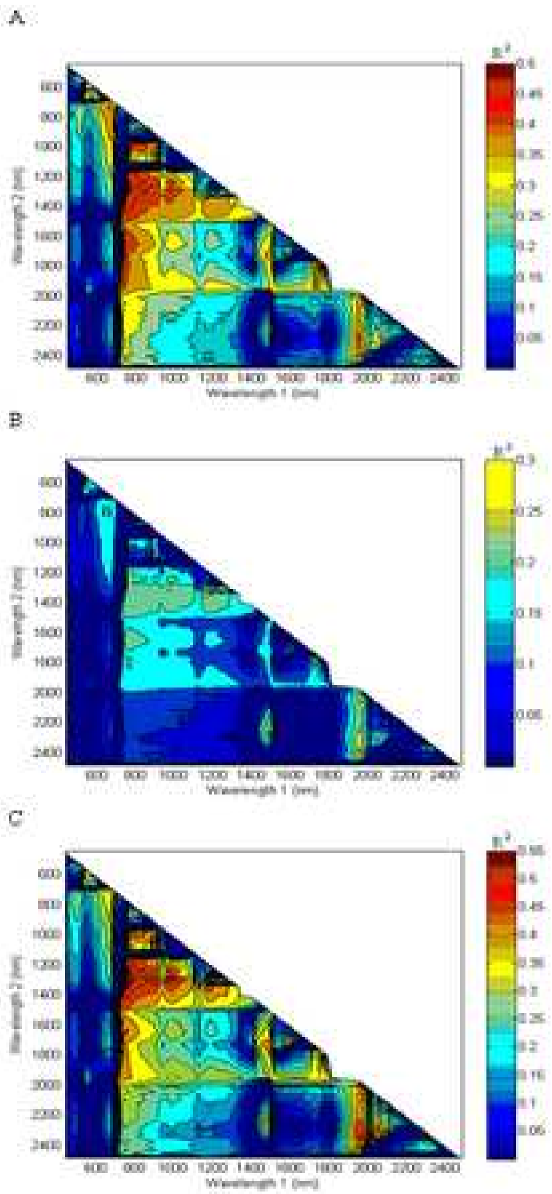

Figure

Click here to download high resolution image

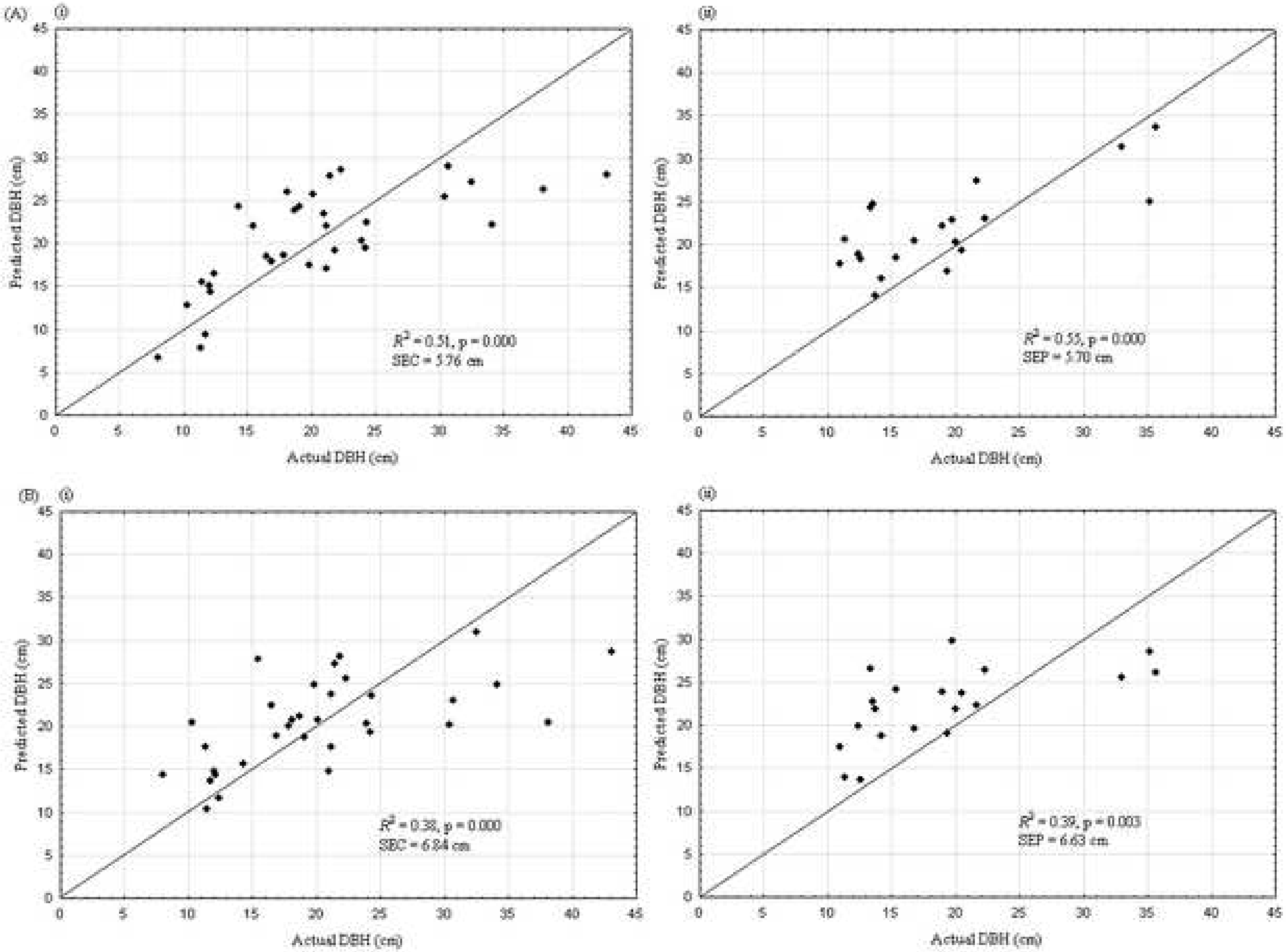

Figure
Click here to download high resolution image

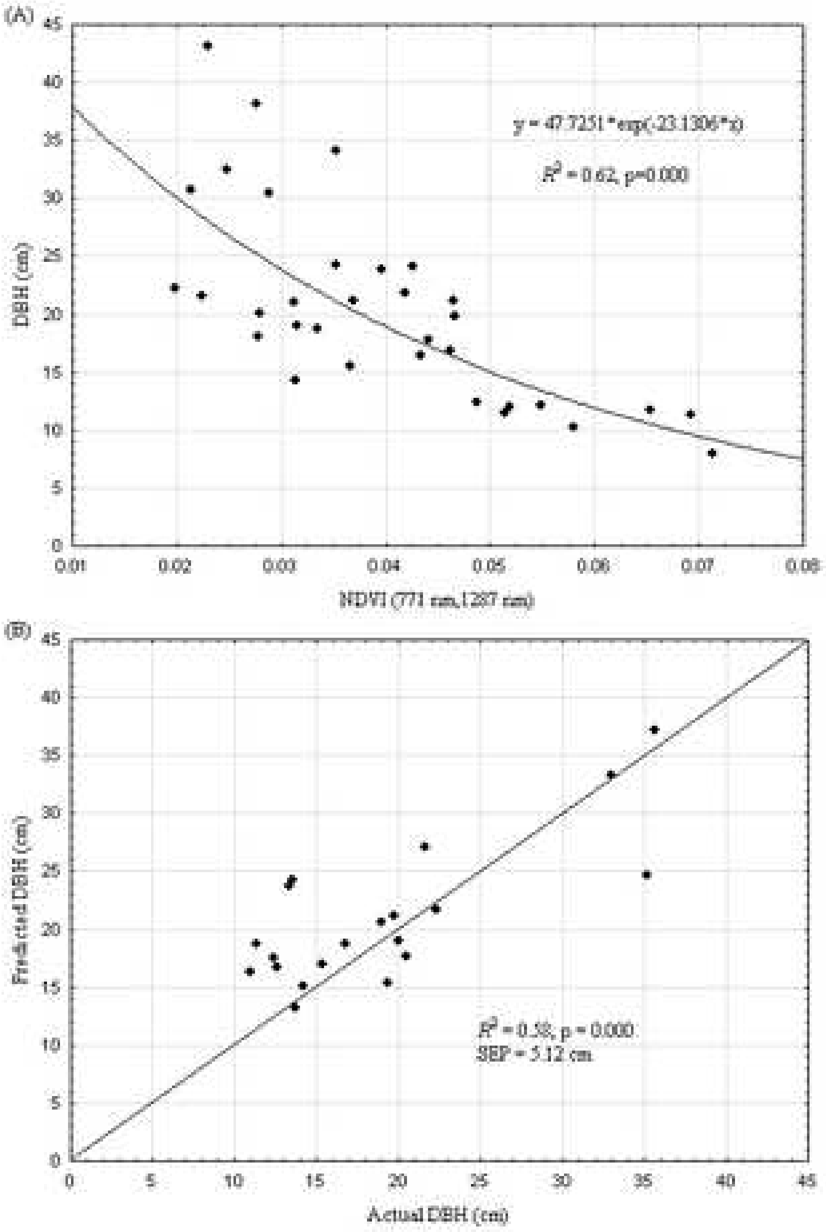

Figure

Click here to download high resolution image

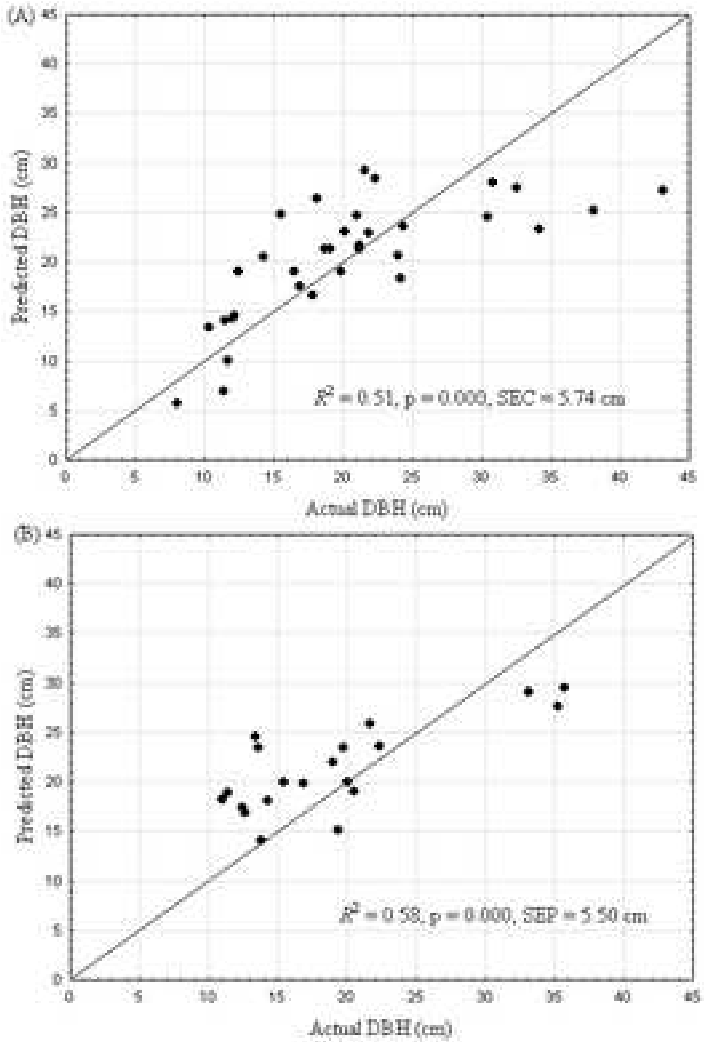

Figure

Click here to download high resolution image

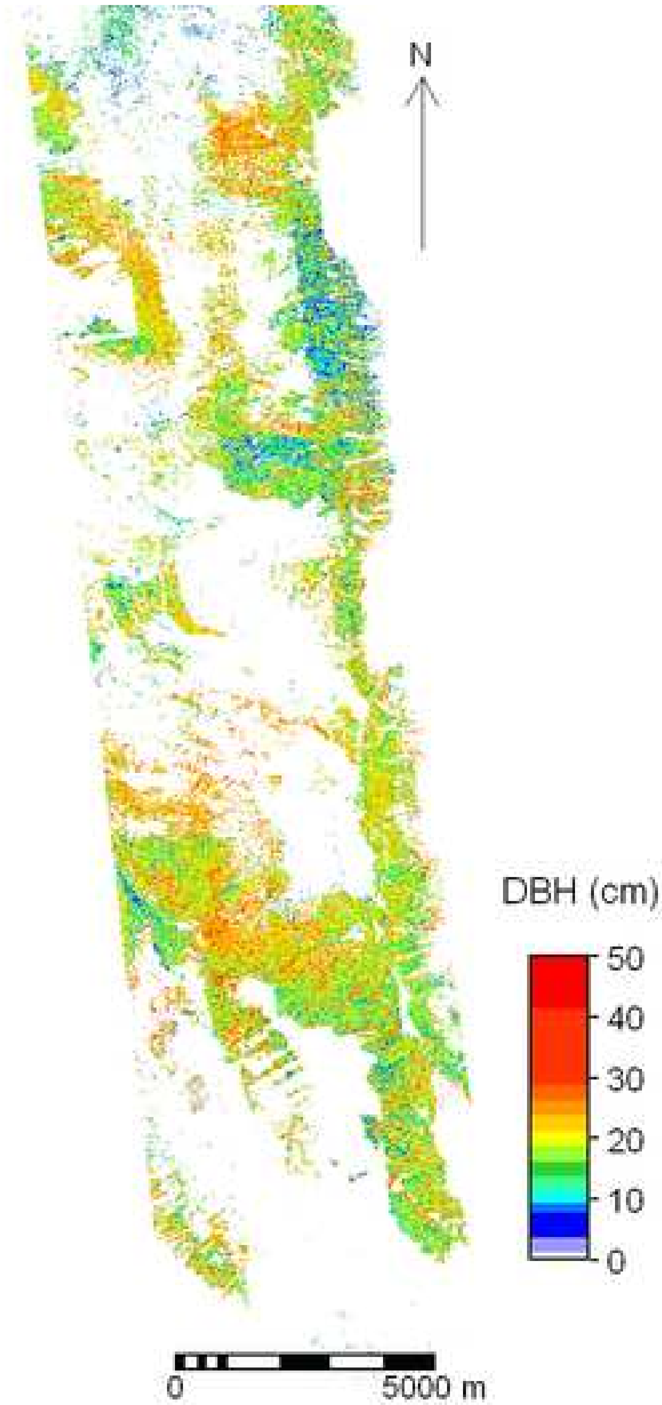

List of tables

Table 1
Wavebands selected for estimating beech forest structural parameters using partial least squares regression (Cho et. al. 2007)

Table 2
Descriptive statistics of beech forest structural parameters. DBH = diameter-at-breast height

Table 3
Best NDVI combinations for predicting beech forest structural parameters (mean diameter-at-breast height (DBH), tree height and density) using linear regression. R^2 = coefficient of determination. The best NDVIs results are compared with those of the standard NDVI involving bands at 831 nm and 665 nm

Table 4
Best NDVI combinations derived from simulated Landsat TM data for predicting beech forest structural attributes (diameter-at-breast height (DBH), tree height and density) using linear regression. R^2 = coefficient of determination

Table 5
Predicting beech forest structural parameters; mean diameter-at-breast-height (DBH), mean height and tree density using partial least squares (PLS) regression. R^2 = coefficient of determination, RMSECV = root mean square error of cross validation, SEC = standard error of calibration and SEP = standard error of prediction

Table 1
Wavebands selected for estimating beech forest structural parameters using partial least squares regression (Cho et. al. 2007)

Waveband centre (nm)	Description	References
466	chlorophyll b	Curran (1989)
695	total chlorophyll	Carter (1994), Gitelson and Merzylak (1997)
725	total chlorophyll, leaf mass	Horler et al. (1983)
740	leaf mass and LAI	Horler et al. (1983)
786	leaf mass	Guyot and Baret (1988)
846	leaf mass, LAI, chlorophyll	Thenkabail et al. (2004)
895	leaf mass, LAI	Thenkabail et al. (2004)
1113	leaf mass, LAI	Thenkabail et al. (2004)
1215	plant moisture, cellulose, starch	Thenkabail et al. (2004), Curran (1989)
1661	lignin, leaf mass, starch	Thenkabail et al. (2004)
2173	protein, nitrogen	Curran (1989)
2359	cellulose, protein, nitrogen	Curran (1989)

LAI = leaf area index

Table 2
Descriptive statistics of beech forest structural parameters. DBH = diameter-at-breast height

Parameter	Mean	Minimum	Maximum	Standard deviation	Skewness	Coefficient of variance (%)
Mean DBH (cm)	19.94	8.00	43.07	8.02	1.01	40
Mean height (m)	18.70	7.00	45.00	7.23	1.35	39
Tree density (No. ha^{-1})	1208	222	3089	739	0.77	61

Table 3
Best NDVI combinations for predicting beech forest structural parameters (mean diameter-at-breast height (DBH), tree height and density) using linear regression. R^2 = coefficient of determination. The best NDVIs results are compared with those of the standard NDVI involving bands at 831 nm and 665 nm.

	Band combinations		Calibration (n = 33)		Validation (n = 20)	
	Band1 (nm)	band 2 (nm)	R^2	SEC	SEP	% mean error
DBH (cm)						
	1287	771	0.51	5.76	5.70	27.8
	1301	771	0.51	5.77	5.69	27.8
	1244	771	0.50	5.78	5.64	27.5
	1258	771	0.50	5.79	5.59	27.3
	1314	771	0.50	5.79	5.72	27.9
	Standard NDVI		0.39	6.42	6.68	32.6
Height (m)						
	1314	1172	0.32	5.75	7.36	39.3
	1301	1172	0.28	5.90	6.70	35.8
	Standard NDVI		0.21	6.19	6.79	36.2
**Density (no. trees/ha)*						
	1301	771	0.59	381	520	48.3
	1287	771	0.58	385	518	48.1
	1314	771	0.58	382	522	48.5
	1230	771	0.57	388	518	48.1
	1244	771	0.57	390	515	47.8
	Standard NDVI		0.37	471	586	54.4

* validation sample size = 17 for tree density. Three outliers eliminated.

Table 4
Best NDVI combinations derived from simulated Landsat TM data for predicting beech forest structural attributes (diameter-at-breast height (DBH), tree height and density) using linear regression. R^2 = coefficient of determination.

Best band combinations		Calibration (n = 33)		Validation (n = 20)	
Band1	band 2	R^2	SEC	SEP	% mean error
DBH (cm)					
1653	831	0.39	7.31	7.27	35.5
831	665	0.38	6.48	6.63	32.4
Height (m)					
1653	831	0.21	6.58	7.22	38.5
831	665	0.20	6.20	6.81	36.4
*Density (no. trees/ha)					
1653	831	0.40	533	581	53.9
831	665	0.36	475	539	50.1

* validation sample size = 17 for tree density. Three outliers eliminated.

Table 5
Predicting beech forest structural parameters; mean diameter-at-breast-height (DBH), mean height and tree density using partial least squares (PLS) regression. R^2 = coefficient of determination, RMSECV = root mean square error of cross validation, SEC = standard error of calibration and SEP = standard error of prediction

	Calibration (n = 33)				Independent validation (n = 20)	
	No. of PLS factors	RMSECV ($g\ m^{-2}$)	R^2	SEC ($g\ m^{-2}$)	SEP ($g\ m^{-2}$)	% of mean
All bands						
DBH (cm)	3	6.56	53	5.63	5.66	27.6
Height (m)	2	6.15	36	5.54	6.12	32.6
Density (no. of trees ha^{-1})	2	461	50	420	508	47.1
Selected bands						
DBH (cm)	3	6.54	51	5.74	5.50	26.8
Height (m)	2	6.16	37	5.52	6.21	33.2
Density (no. of trees ha^{-1})	3	451	50	421	499	46.4